Mn Interstitial Diffusion in (Ga, Mn)As

K. W. Edmonds,[1] P. Bogusławski,[2,3,4] K. Y. Wang,[1] R. P. Campion,[1] S. N. Novikov,[1] N. R. S. Farley,[1] B. L. Gallagher,[1] C. T. Foxon,[1] M. Sawicki,[2,3] T. Dietl,[2,3] M. Buongiorno Nardelli,[4] and J. Bernholc[4]

[1]*School of Physics and Astronomy, University of Nottingham, Nottingham NG7 2RD, United Kingdom*
[2]*Institute of Physics, Polish Academy of Sciences, 02668 Warszawa, Poland*
[3]*ERATO Semiconductor Spintronics Project, Japan Science and Technology Corporation, 02668 Warszawa, Poland*
[4]*Department of Physics, North Carolina State University, Raleigh, North Carolina 27695, USA*

(Received 24 June 2003; published 20 January 2004)

We present a combined theoretical and experimental study of the ferromagnetic semiconductor (Ga, Mn)As which explains the remarkably large changes observed on low-temperature annealing. Careful control of the annealing conditions allows us to obtain samples with ferromagnetic transition temperatures up to 159 K. *Ab initio* calculations, *in situ* Auger spectroscopy, and resistivity measurements during annealing show that the observed changes are due to out diffusion of Mn interstitials towards the surface, governed by an energy barrier of 0.7–0.8 eV. Electric fields induced by Mn acceptors have a significant effect on the diffusion.

DOI: 10.1103/PhysRevLett.92.037201 PACS numbers: 75.70.Ak, 61.72.Cc, 71.15.Nc

The III-V dilute magnetic semiconductors (DMS), in which high levels of transition metal impurities are incorporated into a semiconductor host, offer good prospects for the integration of ferromagnetic properties into semiconductor heterostructures [1]. In DMS a long-range ordering of the magnetic dopants is mediated by the charge carriers, leading to the possibility of spin engineering by carrier manipulation [2,3]. Interest in these materials was further stimulated by predictions of ferromagnetism at room temperature and above [4]. Many of the physical properties of DMS materials have been successfully explained within the Zener mean-field model [4–6], which predicts a Curie temperature T_C determined by the concentration of holes p, and roughly proportional to $p^{1/3}$.

(Ga, Mn)As provides a valuable test ground for DMS properties, due to the relatively high T_C and its compatibility with the well-characterized GaAs system. The Mn dopant substitutes for the Ga site, and fulfills two roles: it provides a local spin 5/2 magnetic moment, and acts as an acceptor, providing itinerant holes which mediate the ferromagnetic order. Practical applications of this material will require an increased control of T_C. An important breakthrough was the discovery that annealing at temperatures close to the growth temperature can result in dramatic enhancements of T_C and p, as well as the saturation magnetization [7–11]. (Ga, Mn)As is grown at relatively low substrate temperatures ($\sim$ 200–250 °C) in order to achieve above equilibrium concentrations of Mn. This tends to lead to high defect concentrations, the most important being Mn interstitials, Mn_I, which are double donors that compensate holes provided by substitutional Mn_{Ga}. The increase of T_C may therefore be related to a removal of these defects. Indeed, ion channeling experiments have indicated a decreased concentration of Mn_I in the annealed material [9]. However, the underlying mechanism giving such large changes at temperatures as low as 180 °C [11] was not previously understood.

Here we report on a combined experimental and theoretical study of the annealing processes in (Ga, Mn)As. *In situ* monitored resistivity measurements as a function of film thickness are shown to be consistent with out diffusion of compensating defects. Using *ab initio* analysis we elucidate possible pathways for Mn_I diffusion, considering the effect of Mn_{Ga}-Mn_I complexes and electric fields induced by the high concentrations of Mn_{Ga} acceptors. The calculated energy barrier agrees with our measured value of 0.7 ± 0.1 eV. These results offer new insights into the detailed microscopic behavior of III-V DMS and the optimization of material properties.

The $Ga_{1-x}Mn_xAs$ films are grown on GaAs(001) substrates by low-temperature ($\approx$ 200 °C) molecular beam epitaxy [12]. The Mn concentration is $x = 0.067$ [13], which was found to give the highest values of T_C [11]. Postgrowth annealing is performed while simultaneously measuring the electrical resistance in a van der Pauw geometry. T_C is obtained from extraordinary Hall effect measurements and from the temperature dependence of the remnant magnetization measured by SQUID magnetometry. The two methods give the same values for T_C within 2 K.

The *in situ* monitored resistivity during annealing at 190 °C is shown in Fig. 1(a), for films of thickness 10 to 100 nm. Initially, the as-grown samples have the same resistivity within 10%. The resistivity then falls as the samples are annealed. A decrease of the resistivity of (Ga, Mn)As films is typically observed on low-temperature annealing [7–11]. This is predominantly due to an increase of the carrier density (the carrier density increases by a factor $\sim$2 for $x = 0.067$, while mobility changes are $\leq$ 10% [10]). The resistivity falls more rapidly with decreasing film thickness, indicating that

 © 2004 The American Physical Society

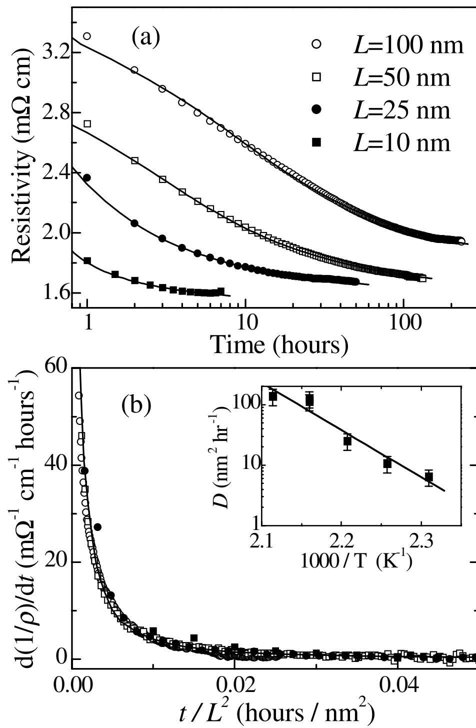

FIG. 1. (a) *In situ* monitored resistivity versus annealing time t, for $Ga_{0.933}Mn_{0.067}As$ films of thickness $L = 100$ nm (open circles), 50 nm (open squares), 25 nm (closed circles), and 10 nm (closed squares), as well as fits using a 1D diffusion model; (b) rate of change of conductivity versus t/L^2 for the data in (a); inset of (b): diffusion coefficient versus $1/T$, for temperature T between 160 and 200 °C.

the ability to deactivate compensating defects is a strong function of the thickness. This suggests that diffusion of Mn_I to the surface or into the substrate is the dominant mechanism in removing the defects.

The data of Fig. 1(a) can be interpreted in terms of one-dimensional out diffusion of mobile compensating defects from a layer of thickness L. The defect density at depth x, time t is given by [14]

$$n'(x, t) = \frac{N}{L}(4\pi Dt)^{-0.5} \int_{-L/2}^{L/2} \exp\left(\frac{-(x - x')^2}{4Dt}\right)dx',$$

where N is the total number of defects per unit area and D the diffusion coefficient. The number of defects per unit area within the layer at time t is then

$$n(t) = \int_{-L/2}^{L/2} n'(x, t)dx.$$

If the change in resistivity is entirely due to the increase in carrier concentration caused by the removal of compensating Mn_I, the time-dependent resistivity can be modeled using

$$\rho(t) = [\sigma_0 - \sigma_1 n(t)]^{-1}$$

with σ_0, σ_1, and D as fit parameters. The model reproduces the experimental data shown in Fig. 1(a). In Fig. 1(b) the rate of change of conductivity, $d(1/\rho(t))/dt$, is plotted versus t/L^2. The data for different thicknesses fall on a single universal curve, which is in excellent agreement with this 1D diffusion picture.

Annealing at different temperatures allows us to determine the temperature dependence of the diffusion coefficient, and thus the energy barrier Q governing the diffusion process, from $D = D_0 \exp(-Q/kT)$. The 25 nm (Ga, Mn)As films from the same wafer were annealed at temperature T from 160 to 200 °C, while monitoring the resistivity *in situ* as above. The value of D obtained from the above fitting procedure is plotted versus 1/T in the inset of Fig. 1. From this we obtain $Q = 0.7 \pm 0.1$ eV.

In practice, diffusion into the substrate is likely to be limited by electrostatics, as a *p-n* junction will eventually form between ionized Mn_I donors and Mn_{Ga} acceptors. In contrast, diffusion to the surface will lead to Mn_I passivation by, e.g., oxidation, so this is the most likely mechanism for removal of Mn_I; its efficiency may depend on the surface orientation and the presence of surface defects. To test this, a 50 nm (Ga, Mn)As sample was grown and transferred to a separate Auger electron spectroscopy chamber, without breaking vacuum. The sample was held in the chamber for several hours to stabilize against gradual oxidation or nitridation of the surface, and then annealed at 240 °C for 40 min. Auger spectra before and after annealing are shown in Fig. 2(a). The Mn Auger signal more than doubles after annealing, consistent with a picture of Mn_I surface accumulation. Low-temperature annealing will therefore be inefficient in (Ga, Mn)As films with capping layers, as has been observed [15].

The remnant magnetization along the in-plane [110] direction versus temperature for the annealed 25 nm

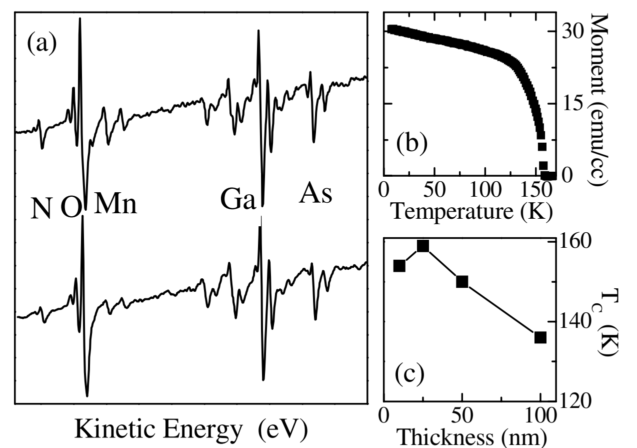

FIG. 2. (a) Auger spectroscopy of (Ga, Mn)As before (below) and after (above) annealing, with features corresponding to N, O, Mn, Ga, and As marked; (b) remnant magnetization versus temperature for 25 nm thick (Ga, Mn)As after annealing; (c) thickness dependence of T_C in the annealed samples.

sample is shown in Fig. 2(b). This is Brillouin-like with a rapid falloff close to T_C, consistent with high homogeneity; however, such measurements can be strongly influenced by the temperature-dependent magnetic anisotropy [16]. As shown in Fig. 2(c), T_C is only weakly thickness dependent, and is significantly above 110 K even for the 100 nm film. Increasing the thickness increases the required anneal time quadratically, so the strong thickness dependence of T_C reported elsewhere [8] may simply be due to incomplete out diffusion in the thicker layers.

We now compare the experimental results with *ab initio* calculations. These are performed within the local spin density approximation, using the plane wave code developed in Trieste [17]. We use a large unit cell with 64 atoms in the ideal case. Thus, substitution of one Ga atom by Mn corresponds to the alloy containing 3.1% of Mn, etc. The Brillouin zone summations, performed using the Monkhorst-Pack scheme with four points in the irreducible part of the ideal *folded* Brillouin zone, give convergent results. Positions of all atoms in the unit cell are allowed to relax, which is particularly important for a correct evaluation of diffusion barriers. In actual samples all Mn_I double donors are ionized to the charge state $2+$, since the Mn_I concentration is significantly lower than that of Mn_{Ga}. Accordingly, in the calculations the Fermi level is fixed to reflect this situation.

In the zinc blende structure there are two interstitial sites with tetrahedral coordination, the first of which, T_{Ga}, is surrounded by four Ga atoms, and the second, T_{As}, by four As atoms. Both sites are shown in the inset of Fig. 3. The electronic structure of Mn_I at both sites is very similar, and the results for T_{As} agree well with those in Ref. [18]. In both locations Mn_I is a double donor. Interstitial diffusion proceeds along ...-T_{Ga}-T_{As}-T_{Ga}-... paths. By symmetry, it is sufficient to investigate one such segment. The calculated changes in the total energy of Mn_I as a function of its position along the T_{Ga}-T_{As} path are presented in Fig. 3. The equilibrium position of an isolated Mn_I^{2+} is the T_{As} site, where its energy is lower than at T_{Ga} by 0.35 eV. The stabilization of Mn_I at the T_{As} site is due to the fact that the positively charged Mn_I^{2+} is attracted by negatively charged As anions, and repelled by positively charged Ga cations. Other aspects of diffusion discussed in the following are also largely determined by Coulomb interactions of Mn_I with acceptors, anions, and cations. The calculated energy barrier for diffusion of Mn_I^{2+} is 0.8 eV, in good agreement with the measured value.

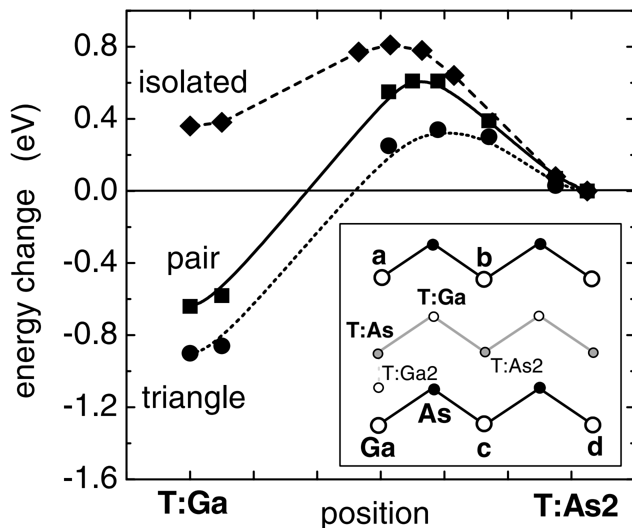

FIG. 3. Calculated changes of the total energy of Mn_I along the T_{Ga}-T_{As} path for isolated Mn_I, Mn_I-Mn_{Ga} pair, and Mn_{Ga}-Mn_I-Mn_{Ga} triangle. Inset: Projection of atomic positions on the (110) plane.

Since there exists a Coulomb attraction between ionized donors and acceptors, we also considered formation of Mn_I-Mn_{Ga} pairs and Mn_{Ga}-Mn_I-Mn_{Ga} complexes. They are coupled by both Coulomb and magnetic interactions. The formation of stable pairs may in principle render the annealing less efficient and block the out diffusion of Mn_I. We first examine the binding of these complexes. If the Mn_{Ga} occupies the site (a) in the inset of Fig. 3, then there are two configurations of the Mn_I-Mn_{Ga} NN pair which have the same energy, with Mn_I occupying the T_{Ga} or the T_{As} site, respectively. There are four T_{Ga} and six T_{As} NN sites. The energy barrier between the two sites is small, 0.5 eV, so that Mn_I will frequently swap between them even at room temperature. Therefore, two possible dissociation paths for the Mn_I-Mn_{Ga} pair exist. They correspond to a jump of Mn_I^{2+} from T_{Ga} to T_{As2}, and from T_{As} to T_{Ga2} in Fig. 3, respectively. These jumps may be regarded as activation of the NN pair dissociation. The total energy change along both paths is shown in Fig. 3, assuming an antiferromagnetic orientation of the Mn pair (see below). The corresponding energy barriers are 1.3 and 1.1 eV.

The geometry analyzed above corresponds to a good approximation to the case of an isolated Mn_{Ga}, because of the relatively large distances between Mn_{Ga} ions in the 64-atom unit cell. On the other hand, our samples contain 6.7% of Mn, and in this case there are on average 2 Mn_{Ga} per 64 atoms. As we will now show, electric fields induced by this high density of acceptors lower the diffusion barriers. We first assume that ionized Mn_{Ga} ions avoid each other. Accordingly, we place Mn_{Ga} as far apart as possible in our 64-atom cubic cell [sites (a) and (d) in Fig. 3]. Because of the presence of the second acceptor at site (d), the calculated barrier along the path T_{Ga}-T_{As2} is reduced from 1.3 to 1.0 eV. Moreover, the distances of Mn_I at T_{As2} to sites (a) and (d) are equal, which implies an equal Coulomb attraction by both acceptors. If the second Mn_{Ga} acceptor is located somewhat closer [e.g., at site (c)], the dissociation barrier along the T_{Ga}-T_{As2} path is reduced even more. A similar decrease of the barrier by about 0.2 eV is expected for the T_{As}-T_{Ga2} path.

In the opposite limit, two Mn_{Ga} atoms are located close to each other, at sites (a) and (b) in Fig. 3. In a stable complex, a Mn_{Ga}-Mn_I-Mn_{Ga} triangle is formed, with Mn_I at T_{Ga}. In the first step of dissociation, Mn_I jumps from T_{Ga} to T_{As2} with a barrier of 1.25 eV. The subsequent jumps to more distant sites require overcoming barriers of about 1.1 eV.

In actual samples, Mn_{Ga} ions are distributed randomly, and the diffusion has the character of a percolation process with a spread of energy barriers. A more detailed treatment of this complex problem is beyond the scope of this Letter. However, it is clear that the electric fields induced by a high density of acceptors lower the activation barrier for diffusion from 1.1 to 0.9 ± 0.1 eV, leading to satisfactory agreement with the measured value of 0.7 ± 0.1 eV.

To evaluate the magnetic coupling of the Mn_{Ga}-Mn_I pair we compare the energies of the ferromagnetic (FM) and antiferromagnetic (AF) orientations of the magnetic moments. For both T_{Ga} and T_{As} locations of Mn_I, the energy difference between the two orientations, ΔE^{A-F}, is -0.5 eV, which corresponds to an AF interaction. This AF character has been anticipated based on model calculations [19]. The coupling has a short-range character, since ΔE^{A-F} vanishes for the second NN (i.e., for T_{As2} or T_{Ga2} sites) and more distant pairs. This behavior is in sharp contrast to the long-range interaction between a pair of substitutional Mn ions. For the Mn_{Ga}-Mn_I-Mn_{Ga} triangle, in the magnetic ground state the moments of the two substitutional Mn_{Ga} are parallel, while the orientation of the Mn_I moment is antiparallel, in agreement with the AF Mn_{Ga}-Mn_I coupling. The FM orientation of the three magnetic moments of the complex is 0.65 eV higher in energy. AF coupling of a significant fraction of Mn_I and Mn_{Ga} may explain why the measured moment of (Ga, Mn)As is often smaller than the predicted value of $4\mu_B$ per Mn [20], and why this increases on removing Mn_I by annealing [7].

Finally, and importantly, the kick-out mechanism of diffusion ($Mn_I + Ga_{Ga} \rightarrow Mn_{Ga} + Ga_I$) is inefficient, since the calculated barrier is about 3 eV.

It can be expected that self-compensation by mobile defects discussed here is a common feature of arsenides and antimonides with ferromagnetism controlled by band carriers. For example, the recently observed increase of T_C to 125 K in (Ga, In, Mn)As upon annealing [21] is most likely due to the mechanism discussed here. Considering (Ga, Mn)N, a consistent picture of magnetism in this material is still lacking. The reported Mn-Mn coupling is either antiferromagnetic, leading to a spin-glass phase, or ferromagnetic, with T_C exceeding 300 K and involving typically less than 20% of Mn spins [22]. Since self-compensation is of prime importance in nitrides [23], one may speculate that the high mobility of compensating defects may favor the formation of ferromagnetic clusters, thus explaining why only some of the localized spins participate in ferromagnetism in such systems.

In summary, a combined experimental and theoretical study of (Ga, Mn)As films has demonstrated that the strong increase of the Curie temperature (up to 159 K), hole density, and saturation magnetization result from an out diffusion of compensating donors towards the surface, identified here as Mn interstitial defects. The diffusion is affected by electric fields of ionized Mn acceptors. The effective diffusion barrier is about 0.7–0.8 eV.

We thank Z. Wilamowski and J. L. Dunn for enlightening discussions. This work is supported by FENIKS project (EC:G5RD-CT-2001-00535), Grant No. PBZ-KBN-044/P03/2001, CELDIS EC:ICA1-CT-2000-70018 project, and grants from U.S. ONR and DoE.

[1] Y. Ohno *et al.*, Nature (London) **402**, 790 (1999).
[2] H. Ohno *et al.*, Nature (London) **408**, 944 (2000).
[3] S. Koshihara *et al.*, Phys. Rev. Lett. **78**, 4617 (1997).
[4] T. Dietl *et al.*, Science **287**, 1019 (2000).
[5] T. Dietl, H. Ohno, and F. Matsukura, Phys. Rev. B **63**, 195205 (2001).
[6] T. Jungwirth *et al.*, Appl. Phys. Lett. **83**, 320 (2003).
[7] T. Hayashi *et al.*, Appl. Phys. Lett. **78**, 1691 (2001); S. J. Potashnik *et al.*, *ibid.* **79**, 1495 (2001).
[8] K. C. Ku *et al.*, Appl. Phys. Lett. **82**, 2302 (2003); B. S. Sorensen *et al.*, *ibid.* **82**, 2287 (2003).
[9] K. M. Yu *et al.*, Phys. Rev. B **65**, 201303 (2002).
[10] K.W. Edmonds *et al.*, Appl. Phys. Lett. **81**, 3010 (2002).
[11] K.W. Edmonds *et al.*, Appl. Phys. Lett. **81**, 4991 (2002).
[12] R. P. Campion *et al.*, J. Cryst. Growth **247**, 42 (2003).
[13] Secondary ion mass spectrometry measurements show that the Mn is evenly distributed in the as-grown films, and that the Mn densities estimated in Refs. [10–12] are low by $(12 \pm 5)\%$.
[14] B. Tuck, *Atomic Diffusion in III-V Semiconductors* (IOP, Bristol, 1988).
[15] D. Chiba *et al.*, Appl. Phys. Lett. **82**, 3020 (2003); M. B. Stone *et al.*, Appl. Phys. Lett. **83**, 4568 (2003).
[16] M. Sawicki *et al.*, J. Supercond. **16**, 7 (2003).
[17] S. Baroni, A. Dal Corso, S. de Gironcoli, and P. Giannozzi, http://www.pwscf.org.
[18] F. Máca and J. Mašek, Phys. Rev. B **65**, 235209 (2001); S. C. Erwin and A. G. Petukhov, Phys. Rev. Lett. **89**, 227201 (2002).
[19] J. Blinowski and P. Kacman, Phys. Rev. B **67**, 121204 (2003).
[20] P. A. Korzhavyi *et al.*, Phys. Rev. Lett. **88**, 187202 (2002).
[21] S. Ohya, H. Kobayashi, and M. Tanaka, Appl. Phys. Lett. **83**, 2175 (2003).
[22] T. Dietl, Phys. Status Solidi B **240**, 433 (2003), and references cited therein.
[23] P. Bogusławski, E. L. Briggs, and J. Bernholc, Phys. Rev. B **51**, 17 255 (1995).